

A sterile neutrino search at NEOS Experiment

Y.J. Ko,¹ B.R. Kim,² J.Y. Kim,³ B.Y. Han,⁴ C.H. Jang,¹ E.J. Jeon,⁵ K.K. Joo,² H.J. Kim,⁶ H.S. Kim,³ Y.D. Kim,^{5,3,7} Jaison Lee,^{5,*} J.Y. Lee,⁶ M.H. Lee,⁵ Y.M. Oh,^{5,†} H.K. Park,^{5,7} H.S. Park,⁸ K.S. Park,⁵ K.M. Seo,³ Kim Siyeon,¹ and G.M. Sun⁴

(NEOS Collaboration)

¹Department of Physics, Chung-Ang University, Seoul 06974, Korea

²Department of Physics, Chonnam National University, Gwangju 61186, Korea

³Department of Physics and Astronomy, Sejong University, Seoul 05006, Korea

⁴Neutron Science Division, Korea Atomic Energy Research Institute, Daejeon 34057, Korea

⁵Center for Underground Physics, Institute for Basic Science, Daejeon 34047, Korea

⁶Department of Physics, Kyungpook National University, Daegu 41566, Korea

⁷University of Science and Technology, Daejeon 34113, Korea

⁸Korea Research Institute of Standards and Science, Daejeon 34113, Korea

(Dated: June 13, 2022)

An experiment to search for light sterile neutrinos was performed at a reactor with a thermal power of 2.8 GW located at the Hanbit nuclear power complex. The search was done with a detector consisting of a ton of Gd-loaded liquid scintillator in a tendon gallery approximately 24 m from the reactor core. The measured antineutrino event rate is 1965 per day with a signal to background ratio of about 23. The shape of the antineutrino energy spectrum obtained from eight-month data-taking period is compared with a hypothesis of oscillations due to active-sterile antineutrino mixing. It is found to be consistent with no oscillation. An excess around 5 MeV prompt energy range is observed as seen in existing longer baseline experiments. Most of the allowed parameter space of $\Delta m_{41}^2 \leq 4 \text{ eV}^2$ range for a previously reported reactor antineutrino anomaly, is excluded with a confidence level higher than 95%.

PACS numbers: 23.40.-s, 21.10.Tg, 14.60.Pq, 27.60.+j

The mixing among three neutrinos has been well established by experiments performed last two decades since the discovery of neutrino oscillations [1–3]. Consistent measurements of the two mass differences and the three mixing angles of the standard, three-neutrino mixing model have been reported by oscillation experiments using atmospheric, solar, reactor, and accelerator neutrinos [4]. Nevertheless the mass hierarchy, the mass of the lightest neutrino, the Dirac or Majorana nature of the neutrino, and the CP phase are yet to be determined [5].

Even though the number of active light neutrinos is limited to three by Z boson decay-width measurements [6], it is still possible to have additional neutrinos if they are sterile. Sterile neutrinos can be identified by the occurrence of active-sterile neutrino oscillations. A hint for this is the LSND experiment’s report of an observation of $\bar{\nu}_\mu \rightarrow \bar{\nu}_e$ mixing with a frequency corresponding to a mass-squared difference larger than 0.01 eV^2 [7]. Results from the MiniBooNE’s test of the LSND signal are, however, inconclusive [8].

In addition to the LSND result, there are two other anomalies that could possibly be signs of active-sterile neutrino oscillations. An apparent ν_e disappearance over a baseline of a few meters in the GALLEX and SAGE Gallium experiments exposed to radioactive sources was reported [9]; the ratio of the numbers of measured and predicted events is 0.88 ± 0.05 . A number of short baseline reactor antineutrino experiments established limits on the presence of neutrino oscillations with eV mass differences by shape analyses of the measured neutrino energy spectra. Among those experiments, the Bugey experimental limits on sterile neutrinos are the most strin-

gent [10]. Mueller *et al.* [11] found about a 6% deficit in reactor antineutrino event rates compared to the theoretical expectations for the short baseline reactor experiments, which is so called “reactor antineutrino anomaly (RAA).” It can be interpreted as an active-sterile neutrino oscillation with three active neutrinos plus one or more sterile neutrinos, i.e., a $3+n$ scenario [12, 13], compatible with the LSND result. Recent reactor experiments that measured the θ_{13} mixing angle, Daya Bay [14], RENO [15], and Double Chooz [16], all confirmed a similar deficit in the measured neutrino event rates. It is also intriguing that these three experiments observed a significant event excess beyond expectations from existing reactor-flux models [13, 17, 18] at prompt energies around 5 MeV.

The Planck satellite experiment [19] constrained the effective neutrino number less than 3.7 at a 95% confidence level, and excluded the existence of sterile neutrinos with masses near 1 eV fully thermalized in early universe. However, theoretical models such as a large lepton asymmetry [20] or neutrino self-interactions [21] show that the effective number of sterile neutrinos can be much less than one. Therefore, light sterile neutrinos remain compatible with current cosmological constraints and should be searched for in more refined experiments with higher sensitivities. The phenomenology of light sterile neutrinos is recently reviewed in [22].

A search for sterile neutrinos at a nuclear reactor was first proposed by Mikaelyan [23]. Following 3+1 mixing scenario [24], the survival probability of a neutrino with energy E_ν at a distance L shorter than one hundred meter can be approxi-

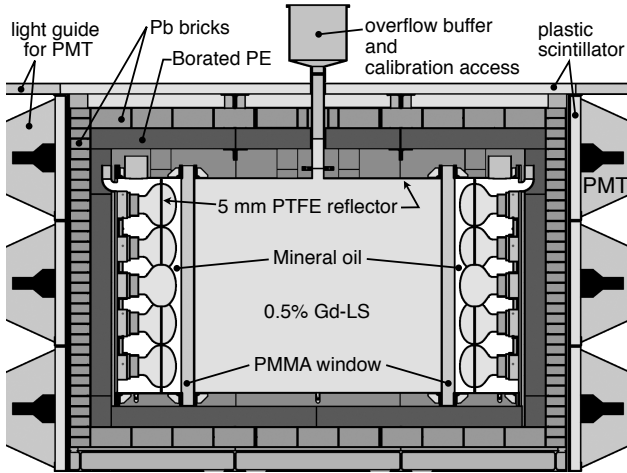


FIG. 1. A simplified cross sectional view of the NEOS detector.

mated as,

$$P \simeq 1 - \sin^2 2\theta_{14} \sin^2 \left(1.27 \frac{\Delta m_{41}^2 L}{E_\nu} \left[\frac{\text{eV}^2 \cdot \text{m}}{\text{MeV}} \right] \right). \quad (1)$$

A new oscillation parameter set of $(\sin^2 2\theta_{14}, \Delta m_{41}^2)$ introduced by existence of an eV-scale light sterile neutrino can be obtained by measuring distortion in the energy spectrum and/or a deficit from expected number of inverse beta decay (IBD, $\bar{\nu}_e + p \rightarrow e^+ + n$) events at a short distance from a nuclear reactor core. Considering the IBD energy spectrum which is smoothly peaked at around 3 MeV, the sensitivity for observing $\sim 1 \text{ eV}^2$ mass-squared difference becomes the highest at several meters and falls off as the distance increases. The Daya Bay experiment sets limits on a light sterile neutrino with lower (i.e., $< 1 \text{ eV}^2$) mass-squared differences [25]. Currently, a number of short baseline reactor experiments are being developed [26]. Here we report results from the NEOS (Neutrino Experiment for Oscillation at Short baseline) experiment for a light sterile neutrino search at a distance of 24 m from a reactor core.

The NEOS detector was installed in the tendon gallery of reactor unit 5 of the Hanbit Nuclear Power Complex in Yeonggwang, Korea. This is the same reactor complex being used for the RENO experiment [15]. The active core size of unit 5 is 3.1 m in diameter, 3.8 m in height and contains 177 low-enriched uranium fuel assemblies; about one third of these assemblies are replaced with fresh ones every eighteen months. The tendon gallery is located 10 m below ground level and is directly under the wall of the containment building. The minimum overburden with the ground and building structures corresponds to twenty meter water equivalent. The detector is centered at 23.7 ± 0.3 m from the center of the reactor core, while the distance to the closest neighboring reactor core is 256 m.

The NEOS detector consists of a neutrino target, mineral oil buffers, passive shieldings, muon counters, and supporting structures (see Fig. 1). The positron-annihilation followed

by a neutron capture from an electron antineutrino IBD process is detected in the target, which is a horizontal cylindrical stainless-steel tank with a 1008 L inner volume (103 cm in diameter, 121 cm in length) filled with a 0.5% Gd-doped liquid scintillator [27]. Each end of the target vessel is viewed by nineteen 8-inch photomultiplier tubes (PMTs) that are closely packed in mineral oil buffers. The buffer and target are separated by a 6 cm-thick transparent PMMA window. Plates of 5 mm thick PTFE reflector are installed on the inner wall of target vessel and along the PMT glasses' equator surfaces. The target tank is enclosed by a 10 cm-thick- borated PE and lead layers for shielding neutrons and external gamma rays, respectively. Muon counters made from 5 cm thick plastic scintillators surround the outside of the detector.

The waveforms of all 38 PMTs are digitized and recorded by 500 mega-sampling (MS) per second flash ADC modules, each of which makes an independent trigger decision. Signals from the muon counters are processed by a 62.5 MS/s ADC module. A trigger control board decides the global trigger and synchronizes the ADC modules. A trigger requiring 30 or more PMT signals higher than 6 mV threshold is fully efficient for energies above 400 keV. The trigger rate was about 210 Hz. The detector operated for 46 days with the reactor off (t_{off}) and 180 days with the reactor on (t_{on}).

The detector was calibrated once every week with ^{137}Cs , ^{60}Co , ^{252}Cf , and PoBe sources. Continuous background events from several well known radioactivities are used for additional calibrations. The charge to energy ratio of single gamma ray events shows a non-linear detector response as shown in Fig. 2(a). An empirical function used to describe

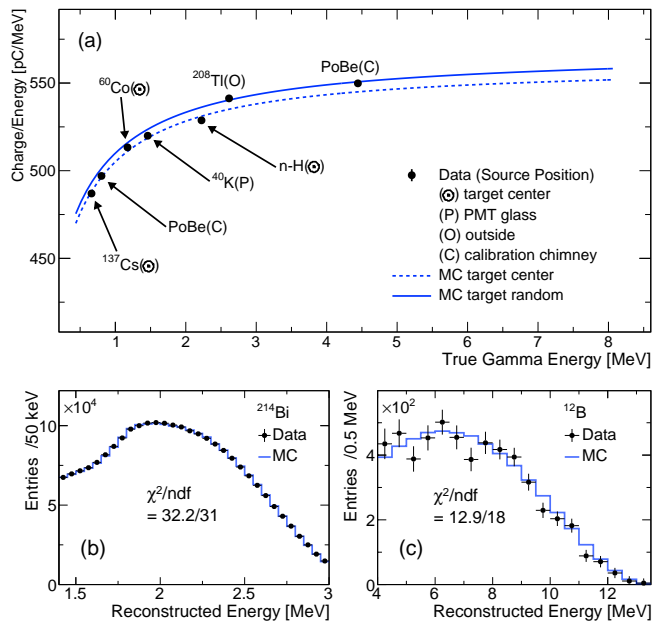


FIG. 2. Detector responses to γ and β sources: (a) ratio of full peak charge to the true γ energy, (b) β -decay spectra for ^{214}Bi , and (c) ^{12}B .

this non-linearity is

$$Q/E_\gamma = (p_0 + p_1 E_\gamma) [1 + p_2 \exp(p_3 \sqrt{E_\gamma})], \quad (2)$$

where Q is the charge, E_γ is the true γ energy, and p_i terms are fitting parameters. The detector stability and the non-uniform response along horizontal axis of the detector are continuously monitored and corrected using 2.6 MeV external γ -rays from ^{208}Ti and internal α background events.

The detector is simulated with a GEANT4-based Monte Carlo simulation (MC). The optical properties of the liquid scintillator and reflecting materials, and responses of PMTs and electronics are fine-tuned to describe the source calibration data and, consequently, the effects of escaping γ -rays, energy resolution ($\sigma/E_\gamma \sim 5\%$ for a full peak at 1 MeV), and the non-linear Q to E_γ response are well reproduced. The reconstructed energy spectra for ^{214}Bi and ^{12}B β -decays are shown in Figs. 2(b) and (c) with the MC results superimposed. The systematic error on the energy scale associated with differences between data and MC is 0.5%.

The selection criteria of IBD candidate events are determined to maximize the signal to background ratio. We start with a pair of events which consists of a prompt event candidate that has energy above 1 MeV and its following delayed event candidate of n -Gd capture signal with energy between 4 and 10 MeV in a 1-30 μs time window. To exclude multiple neutron-induced backgrounds, the pair is rejected when any events occur at a time that is less than 30 μs before or 150 μs after the prompt signal time. Pairs of which the prompt or delayed events occur in a 150 μs interval after a muon-counter hit are vetoed. Finally, pairs caused by the scattering and subsequent capture of fast neutrons are identified using a pulse shape discrimination (PSD) requirement that is adjusted to accept more than 99.9% of the electron-induced recoil events over the full energy range. The background fraction that is removed by the PSD requirement was measured to be 73% during the reactor-off period.

With these requirements, 1965.3 ± 3.3 (80.4 ± 1.3) IBD candidates per day were selected during the reactor-on (-off) period with the prompt energy between 1 and 8 MeV. No evidence was found for additional backgrounds associated with the reactor operation or for significant background fluctuation in the whole running period. The muon-counter rate, to which the fast neutron background is related, was stable at 241 Hz with a 2 Hz day-to-day rms variation. The energy distributions of the fast-neutron scattering events that were rejected by the PSD requirement show only small variations consistent with statistical fluctuations throughout the entire running period. Contributions from accidental background events were estimated by the time-delayed coincidences method [28] to be 7 ± 1 /day, where the error corresponds to the range of the daily variations.

The measured prompt energy spectrum (S_{neos}) is shown in Fig. 3(a), superimposed with the predicted non-oscillation spectra: one based on flux calculations by Huber [13] and Mueller [11] (H-M) weighted by the IBD cross sections [29]

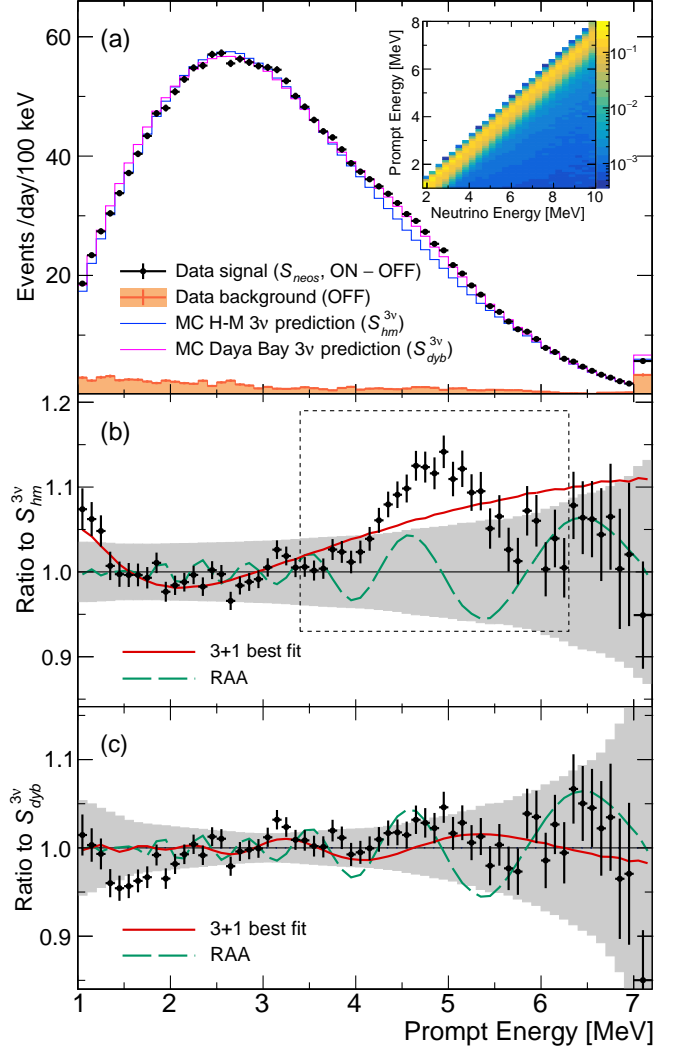


FIG. 3. (a) The IBD prompt energy spectrum. The last bin is integrated up to 8 MeV. Orange shaded histogram is the background spectrum measured during the reactor off period. The detector response matrix in inset shows the relation between the neutrino energy and the prompt energy. (b) The ratio of the observed prompt energy spectrum to the H-M prediction with 3ν hypothesis. Test of oscillation is conducted excluding the data points in the dashed-rectangle. The predicted spectrum is scaled to match the area of the data excluding the same data points. (c) The ratio of the data to the expected spectrum based on the Daya Bay result with 3ν hypothesis, scaled to match the whole area. For (b) and (c), the solid red curves denote the expected oscillation patterns for the best fit of data to the $3+1$ neutrino hypothesis and the corresponding oscillation parameters ($\sin^2 \theta_{14}$, Δm_{41}^2) are $(0.171, 0.163 \text{ eV}^2)$ and $(0.033, 1.32 \text{ eV}^2)$, respectively. The green long-dashed curve is the expected oscillation pattern for the RAA best fit parameters $(0.142, 2.32 \text{ eV}^2)$. The gray error bands are total systematic uncertainties, corresponding to square roots of diagonal elements of the covariance matrices.

and the other based on the Daya Bay reactor antineutrino spectrum [30]. The former and latter predicted spectra are denoted as S_{hm} and S_{dyb} , respectively, and their superscript 3ν (4ν) denotes the 3 ($3+1$) neutrino hypothesis. The predictions are

generated using a full simulation of IBD events of which the $\bar{\nu}_e + p$ reaction occurs at random positions throughout the detector target and produced e^+ and n are propagated through all of the detector responses. The antineutrino is assumed to originate uniformly throughout the active reactor core and the average primary element fission fractions of 0.655, 0.072, 0.235, and 0.038 for ^{235}U , ^{238}U , ^{239}Pu , and ^{241}Pu , respectively, are used. The differences between the fission fractions for the NEOS data and the ones for Daya Bay are taken into account and small corrections are made using the H-M flux model as instructed in Ref. [30].

The excess around 5 MeV versus $S_{hm}^{3\nu}$ is clearly seen, as shown in Figs. 3(a) and (b), for the first time at this short baseline. The excess does not completely disappear even in $S_{neos}/S_{dyb}^{3\nu}$ spectrum, as shown in Fig. 3(c). This can be explained as that the excess can be contributed differently from each fission element [31]. It is, however, difficult to conclude with the current level of uncertainties. Another large discrepancy other than the 5 MeV excess for the $S_{neos}/S_{hm}^{3\nu}$ case is found at the lowest energy range. The disagreement is as large as 8% at 1 MeV and drops rapidly as energy increases. For the $S_{neos}/S_{dyb}^{3\nu}$ case at the same range, the statistical errors touch the systematic error band and the disagreement is rather small. Other small fluctuations at several energies also seem to have some small structures which are common for both reference spectra but, regarding the uncertainties, are not so significant.

Following systematic uncertainties are taken into account. Errors in the reference antineutrino spectra are the main contributors to the total uncertainties. The 0.5% uncertainty in the reconstructed energy scale is another large contributor to the total uncertainty. The statistical fluctuations of the measured background spectrum are assigned as another source of the bin-to-bin uncorrelated uncertainty and their effects are not negligible at the lowest and highest energy range. Other sources of uncertainty, such as the inaccuracy of the effective baseline, fuel related uncertainties from burn-up and fission fractions, spill-in from inactive volumes, events generated by antineutrinos from neighbor reactors, and other detector-related uncertainties have negligible effects on the spectral shape.

Probing signs of an oscillation in a spectrum measured with a single detector at one fixed distance from the reactor core depends on the accuracy and precision of the reference spectrum. Among the available references, the H-M flux model provides bin-to-bin correlated and uncorrelated uncertainties and, even though their uncertainties are underestimated [18], their spectral shape (not their absolute rate) are generally in good agreement with existing experimental results except for the region of the 5 MeV excess. A recent high-resolution *ab initio* calculation by Dwyer *et al.* [17] better describes the observed 5 MeV excess, but its large uncertainties and their correlations, which are yet to be exactly quantified, make a comparison with our data impractical. Experimentally, only the Daya Bay unfolded spectrum [30] is based on a direct measurements and, therefore, the uncertainties in antineutrino spectrum are relatively small. The correlation of uncertainties

among the energy bins can be dealt with the provided covariance matrix.

In the present work, the measured prompt energy spectrum is compared with S_{dyb} and S_{hm} for testing the oscillation. For the comparison with S_{dyb} , all the data in 1-8 MeV prompt energy range are used, while the 5 MeV excess region is excluded for the S_{hm} case. A χ^2 is constructed for each comparison with a covariance matrix V_{ij} that accounts for correlations between uncertainties:

$$\chi^2 = \sum_{i=1}^N \sum_{j=1}^N (M_i - \frac{t_{\text{on}}}{t_{\text{off}}} B_i - T_i) V_{ij}^{-1} (M_j - \frac{t_{\text{on}}}{t_{\text{off}}} B_j - T_j), \quad (3)$$

where M (B) is the number of measured IBD candidate events accumulated during the reactor-on (-off) period, T is the prediction from a reference spectrum that accounts for oscillation parameters, and the subscripts i and j denote the prompt energy bin. To construct V_{ij} , the elements for the errors in antineutrino flux are calculated from the tabulated numbers in Refs. [11, 13] and the matrix in Table 13 of Ref. [30], by convolving them with the detector response shown in the inset of Fig. 3(a). Then the other elements from statistical and detector systematic uncertainties are added.

The χ^2 values are calculated on a fine grid in the sensitive Δm_{41}^2 range from 0.04 eV² to 12 eV². For the S_{dyb} case, the χ^2 value with the 3- ν hypothesis is $\chi_{3\nu}^2/\text{NDF} =$

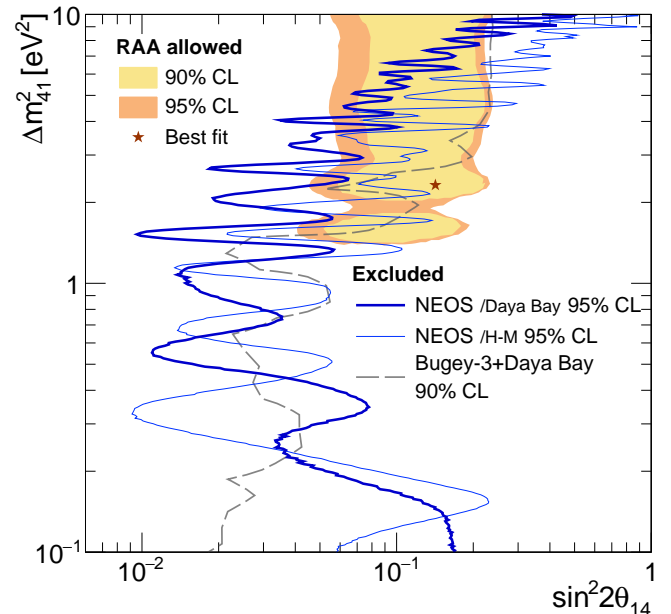


FIG. 4. Exclusion curves for 3+1 neutrino oscillations in the $\sin^2 2\theta_{14} - \Delta m_{41}^2$ parameter space. The thick-blue curve is 95% CL exclusion contours based on the comparison with the Daya Bay spectrum, the thin-blue curve is for comparison with the H-M flux prediction excluding 5 MeV excess. The gray-dashed curve shows the combined Daya Bay and Bugey 90% CL results [32]. The shaded area is the allowed region from the reactor anomaly fit and star is its optimum point [12].

58.4/70, where NDF denotes the number of degrees of freedom. The minimum χ^2 value with the 3+1 hypothesis is $\chi^2_{4\nu}/\text{NDF} = 49.4/68$. The corresponding χ^2 difference, $\Delta\chi^2 = \chi^2_{3\nu} - \chi^2_{4\nu} = 9.0$, shows no significant favor for the 3+1 hypothesis. For the S_{hm} case, the minimum χ^2 value with the 3+1 hypothesis is $\chi^2_{4\nu}/\text{NDF} = 30.9/39$ at $\sin^2 2\theta_{14} = 0.171$, $\Delta m_{41}^2 = 0.163 \text{ eV}^2$, while the 3- ν hypothesis gives $\chi^2_{3\nu}/\text{NDF} = 55.9/41$. It can be seen in Fig. 3(b) that the discrepancy in the low energy range between S_{neos} and $S_{hm}^{3\nu}$ leads to a relatively large $\chi^2_{3\nu}$ value and an oscillation for a low Δm_{41}^2 with a large mixing angle is highly favored. At the same point or in its vicinity for the comparison with S_{dyb} , however, $\Delta\chi^2$ values do not even exceed 1. As a result, no apparent parameter set of $(\sin^2 2\theta_{14}, \Delta m_{41}^2)$ that has significant favor for both $S_{dyb}^{4\nu}$ and $S_{hm}^{4\nu}$ is found. The optimum point for the RAA fit, $(0.142, 2.32 \text{ eV}^2)$ [12] is disfavored in both comparisons, where the corresponding χ^2 values are 112 and 70.7 for the S_{dyb} and S_{hm} cases, respectively.

The limit on the $\sin^2 2\theta_{14}$ value for each Δm_{41}^2 is found using raster scan [33]. For a Δm_{41}^2 value, a probability density function, $f(\sin^2 2\theta_{14})$, is constructed from the $\Delta\chi^2$ distribution in the $\sin^2 2\theta_{14}$ range from 0 to 1, where $\Delta\chi^2$ is the difference between a χ^2 value at a $\sin^2 2\theta_{14}$ point and the minimum χ^2 value at the corresponding Δm_{41}^2 . The upper limit (ul) at confidence level (CL) of $1 - \alpha$ is found with the condition of:

$$\int_{ul}^1 f(\sin^2 2\theta) d(\sin^2 2\theta) = \alpha. \quad (4)$$

The resulting exclusion limits at 95% CL are shown in Fig. 4, superimposed with the 90% CL exclusion curve of Daya Bay/Bugey-3 combined limits from Ref. [32], and with the allowed region by the RAA fit from Fig. 8 in Ref. [12]. From the comparison with S_{dyb} , a larger area is excluded compared to the Daya Bay/Bugey-3 combined result in the high Δm_{41}^2 range up to 10 eV^2 , and most of the allowed space by the RAA fit are excluded for $\Delta m_{41}^2 \leq 4 \text{ eV}^2$. The excluded region from the comparison with S_{hm} is smaller than the region from the S_{dyb} case in high Δm_{41}^2 side, mainly due to a sensitivity loss by ignoring the 5 MeV excess region, but still compatible with the Daya Bay/Bugey-3 result. The fluctuations in S_{neos} compared to the reference spectra make the structures in the exclusion curves.

In conclusion, no strong evidence for 3+1 neutrino oscillations is observed in this study. The most stringent upper limit on the θ_{14} mixing angle for 1-10 eV^2 Δm_{41}^2 region is obtained, thanks to the high signal to background ratio, good energy resolution, and a normalization to the Daya Bay antineutrino spectrum. The new limits exclude a large region of the parameter space of $(\sin^2 2\theta_{14}, \Delta m_{41}^2)$ allowed by the RAA fit at a confidence level higher than 95%. The results are currently limited by uncertainties in the reference spectra taken by Daya Bay and systematics of the NEOS data. The systematic uncertainties in the antineutrino spectrum will be reduced if the reference spectrum comes from the RENO experiment since it uses the same reactor complex. Other on-going

or scheduled experiments [34–37] with even shorter baselines and/or better L/E resolution are expected to improve the sensitivities. It should be remarked that in addition to these short-baseline sterile neutrino searches, future long-baseline reactor anti-neutrino experiments [38, 39] aimed at the determination of the neutrino mass hierarchy would require more accurate reference IBD spectra. Recently, ICE-CUBE and MINOS experiments constrained θ_{24} mixing angle for 3+1 sterile neutrino model [40, 41] and rejected the LSND anomaly parameter space combining θ_{14} limit from reactor antineutrinos [32]. Our new limit will further improve the constraints to the LSND anomaly parameter space by combining with the θ_{24} measurements.

This work is supported by IBS-R016-D1 and 2012M2B2A6029111 from National Research Foundation (NRF). We appreciate the Korea Hydro and Nuclear Power (KHNP) company and especially acknowledge the help and support provided by staff members of the Hanbit-3 Nuclear Power Plant's Safety and Engineering Support Team. We appreciate the Daya Bay collaboration for the discussion on the errors in their reference spectrum.

* Corresponding author : jsahnlee@ibs.re.kr

† Corresponding author : yoomin@ibs.re.kr

- [1] Y. Fukuda *et al.* (Super-Kamiokande), Phys. Rev. Lett. **81**, 1562 (1998).
- [2] Q. R. Ahmad *et al.* (SNO), Phys. Rev. Lett. **89**, 011301 (2002).
- [3] K. Eguchi *et al.* (KamLAND), Phys. Rev. Lett. **90**, 021802 (2003).
- [4] G. L. Fogli, E. Lisi, A. Marrone, D. Montanino, A. Palazzo, and A. M. Rotunno, Phys. Rev. **D86**, 013012 (2012).
- [5] C. Giunti and C. W. Kim, *Fundamentals of Neutrino Physics and Astrophysics* (Oxford University Press, UK, 2007).
- [6] S. Schael *et al.* (SLD Electroweak Group, DELPHI, ALEPH, SLD, SLD Heavy Flavour Group, OPAL, LEP Electroweak Working Group, L3), Phys. Rept. **427**, 257 (2006).
- [7] C. Athanassopoulos *et al.* (LSND), Phys. Rev. Lett. **77**, 3082 (1996).
- [8] A. A. Aguilar-Arevalo *et al.* (MiniBooNE), Phys. Rev. Lett. **110**, 161801 (2013).
- [9] J. N. Abdurashitov *et al.*, Phys. Rev. **C73**, 045805 (2006).
- [10] Y. Declais *et al.*, Nucl. Phys. **B434**, 503 (1995).
- [11] T. A. Mueller *et al.*, Phys. Rev. **C83**, 054615 (2011).
- [12] G. Mention, M. Fechner, T. Lasserre, T. A. Mueller, D. Lhuillier, M. Cribier, and A. Letourneau, Phys. Rev. **D83**, 073006 (2011).
- [13] P. Huber, Phys. Rev. **C84**, 024617 (2011), [Erratum: Phys. Rev. C85, 029901(2012)].
- [14] F. P. An *et al.* (Daya Bay), Phys. Rev. Lett. **116**, 061801 (2016).
- [15] J. H. Choi *et al.* (RENO), Phys. Rev. Lett. **116**, 211801 (2016).
- [16] Y. Abe *et al.* (Double Chooz), Phys. Rev. Lett. **108**, 131801 (2012).
- [17] D. A. Dwyer and T. J. Langford, Phys. Rev. Lett. **114**, 012502 (2015).
- [18] A. C. Hayes, J. L. Friar, G. T. Garvey, G. Jungman, and G. Jonkmans, Phys. Rev. Lett. **112**, 202501 (2014).
- [19] P. A. R. Ade *et al.* (Planck), (2015), arXiv:1502.01589 [astro-

ph.CO].

- [20] J. Hamann, S. Hannestad, G. G. Raffelt, I. Tamborra, and Y. Y. Y. Wong, *Phys. Rev. Lett.* **105**, 181301 (2010).
- [21] S. Hannestad, R. S. Hansen, and T. Tram, *Phys. Rev. Lett.* **112**, 031802 (2014).
- [22] K. N. Abazajian *et al.*, (2012), arXiv:1204.5379 [hep-ph].
- [23] L. Mikaelyan and V. Sinev, *Fundamental interactions of elementary particles. Proceedings, Conference, Moscow, Russia, November 16-20, 1998*, *Phys. Atom. Nucl.* **62**, 2008 (1999), [Yad. Fiz.62,2177(1999)].
- [24] C. Giunti and M. Laveder, *Phys. Rev.* **D84**, 073008 (2011).
- [25] F. P. An *et al.* (Daya Bay), *Phys. Rev. Lett.* **117**, 151802 (2016).
- [26] P. Vogel, L. Wen, and C. Zhang, *Nature Commun.* **6**, 6935 (2015).
- [27] B. R. Kim *et al.*, (2015), arXiv:1511.05551 [physics.ins-det].
- [28] Y. Abe *et al.* (Double Chooz), *Phys. Rev.* **D86**, 052008 (2012).
- [29] P. Vogel and J. F. Beacom, *Phys. Rev.* **D60**, 053003 (1999).
- [30] F. P. An *et al.* (Daya Bay), (2016), arXiv:1607.05378 [hep-ex].
- [31] P. Huber, (2016), arXiv:1609.03910 [hep-ph].
- [32] P. Adamson *et al.* (MINOS, Daya Bay), *Phys. Rev. Lett.* **117**, 151801 (2016).
- [33] L. Lyons, (2014), arXiv:1404.7395 [hep-ex].
- [34] N. Ryder (SoLid), *Proceedings, 2015 European Physical Society Conference on High Energy Physics (EPS-HEP 2015)*, PoS **EPS-HEP2015**, 071 (2015).
- [35] J. Ashenfelter *et al.* (PROSPECT), in *Community Summer Study 2013: Snowmass on the Mississippi (CSS2013)* Minneapolis, MN, USA, July 29-August 6, 2013 (2013) arXiv:1309.7647 [physics.ins-det].
- [36] V. Hlaine, in *NuPhys2015: Prospects in Neutrino Physics (NuPhys)* London, UK, December 16-18, 2015 (2016) arXiv:1604.08877 [physics.ins-det].
- [37] I. Alekseev *et al.*, (2016), arXiv:1606.02896 [physics.ins-det].
- [38] F. An *et al.* (JUNO), *J. Phys.* **G43**, 030401 (2016).
- [39] S.-B. Kim, *Proceedings, Neutrino Oscillation Workshop (NOW 2014)*, *Nucl. Part. Phys. Proc.* **265-266**, 93 (2015).
- [40] M. G. Aartsen *et al.* (IceCube), *Phys. Rev. Lett.* **117**, 071801 (2016).
- [41] P. Adamson *et al.* (MINOS), *Phys. Rev. Lett.* **117**, 151803 (2016).